19th Australasian Fluid Mechanics Conference
Melbourne, Australia
8-11 December 2014

Modelling of Oscillatory Flow around Four Cylinders in a Diamond Arrangement

F. Tong[1], L. Cheng[1, 2], T. Zhou[1]

[1] School of Civil, Environmental and Mining Engineering
The University of Western Australia, 35 Stirling Highway, Crawley, WA 6009, Australia

[2] Stake Key Laboratory of Coastal and Offshore Engineering,
Dalian University of Technology, Dalian, 116024, China

Abstract

This study numerically investigates the features of oscillatory flow around four circular cylinders in diamond arrangements and the forces on the structures. At close distances, the flow field around the four staggered cylinders may resemble that around a single one. It is also observed that at low frequencies of oscillation, the flow field is symmetric to the two inline cylinders; even the proximity interference is strong. However, the flow field is prone to be chaotic due to the asymmetric vortex shedding from each member and the interactions of the shed vortices, and it becomes increasedly unstable with the increased frequency of oscillation, gap distances (to the extent of present study) and amplitude of oscillation. The two inline cylinders generally experience low drag and inertial force coefficients compared to that of two side cylinders, partially due to the wake shielding effect.

Introduction

The sinusoidally oscillating flows around a circular cylinder have been an interest of fluid mechanics for decades, due to the ocean engineering applications [3] as well as the rich flow mechanism it presents [4], such as wave loads on ocean structures and when or how the vortices are generated and shed from the structure. Despite the fact that cylindrical structures commonly appear in bundle in engineering applications, the study on oscillating flow around multiple circular cylinders is scarce. It has been observed that the interactions of flows around two cylinders in tandem/side-by-side [6] and around four cylinders in an inline array [5] lead to much more complex flow features than those in the wake of a single cylinder. It is expected that an array of four cylinders in a diamond arrangement, as shown in figure 1(a), which involves cylinder arrangements in tandem, side-by-side as well as staggered, must share similar flow interferences and present even more flow dynamics. However, this kind of flow is limitedly covered by previous studies [2].

The behavior of flow fields around a circular cylinder is controlled by two dimensionless parameters, the Keulegan-Carpenter number, *KC*, and the Reynolds number, Re, which are defined as $KC = U_m T/D$ and $\mathrm{Re} = U_m D/\nu$, respectively, where D is the diameter of the cylinder, ν is the kinematic viscosity of the fluid, U_m is the maximum velocity and T is the oscillating period. The ratio of Re and *KC* is referred as the frequency parameter or Stokes number, $\beta = \mathrm{Re}/KC$. Comprehensive flow features induced by sinusoidal oscillations of a circular cylinder in otherwise stationary fluid at low *KC* and low β were experimentally identified by Tatsuno and Bearman [4] and classified into eight fascinating flow regimes.

There is no doubt that the flow dynamics around a cylinder array are greatly influenced by the distances among the cylinders and the alignment angle of this array to the direction of the oscillating flow, in addition to *KC* and Re. To explore the influences, this work presents a study on the sinusoidally oscillatory flow around a four-cylinder array in diamond arrangements, by solving the two-dimensional Navier-Stokes equations directly using a finite volume method. Three spacing ratios (G) from 1 to 3 are examined, where G is defined in figure 1(a) as $G = L/D$, with L being the gap distance between two neighbour cylinders. Numerical simulations are carried out at relatively low frequencies and amplitudes of oscillations within $KC \in [1, 12]$ and Re = 150&200, where it is believed that two-dimensional (2-D) numerical method is validated to capture the sectional flow features [5] [6]. Our scope is to identify the flow regimes of the four-staggered cylinders in comparison with that of a single one and to investigate how the flow field is dependent on *G*, *KC* and Re. Due to the wake and proximity interferences, a variety of distinct flow patterns and diverse force features are expected.

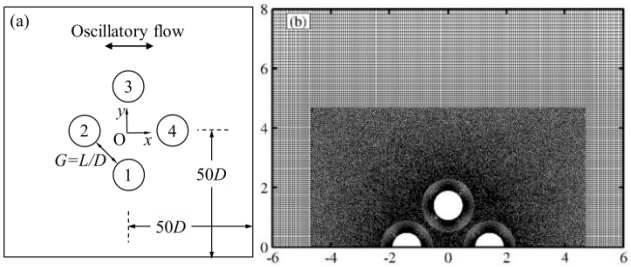

Figure 1. Schematic representation and mesh distributions of the four circular cylinder system. (a) computational domain. (b) view of the mesh surrounding the cylinders, which consist of layers of structured quadrilateral cells from cylinder surfaces, followed by unstructured triangular cells in near fields and structured cells in the far fields.

Numerical Methods

Oscillatory flow around the four-cylinder system shown in figure 1(a) is simulated by solving the 2-D Navier-Stokes (NS) equations. The dimensionless form of 2-D NS equations for incompressible flow in the Cartesian coordinate system can be expressed as [1],

$$\frac{1}{KC}\frac{\partial \vec{U}}{\partial t} + \nabla \cdot \left(\vec{U}\vec{U}\right) - \frac{1}{\mathrm{Re}}\nabla^2 \vec{U} + \nabla p = 0 \qquad (1)$$

$$\nabla \cdot \vec{U} = 0 \qquad (2)$$

where the velocity $\vec{U}$ has two components U_x and U_y in the x- and y-directions, respectively, t is time, and p is hydrodynamic pressure. The NS equations are solved using the Open source Field Operation and Manipulation (OpenFOAM®) C++ libraries, which is a free source CFD package developed by OpenCFD Ltd. The finite volume method is used in the solver and the pressure-velocity coupling is achieved following the Pressure Implicit with Splitting of Operators (PISO) method. The convection terms are discretised using the Gauss cubic scheme, while the Laplacian and the pressure terms in the momentum equations are

discretised using the Gauss linear scheme. Euler implicit scheme is adopted for the temporal discretisation.

A relatively large rectangular computational domain ($100D \times 100D$) similar to that shown in figure 1(a) is employed in this study, with the cylinder array being placed at the centre of the domain. The initial values for flow velocity and pressure in the whole domain are set to be zero. Flow velocity on the left boundary is specified as

$$U_x(t) = U_m \sin\left(\frac{2\pi}{T}t\right) \quad (3)$$

The pressure and the velocity gradients in the *x*-direction are set to be zero at the right boundary and the symmetric boundary conditions are applied at the two lateral boundaries that are parallel to the flow directions. The no-slip boundary condition is adopted on the cylinder surfaces. Figure 1 (b) illustrates the mesh distribution of the cylinder system. The computational domain and mesh sizes were determined through a domain and mesh size dependency check, which is not detailed here.

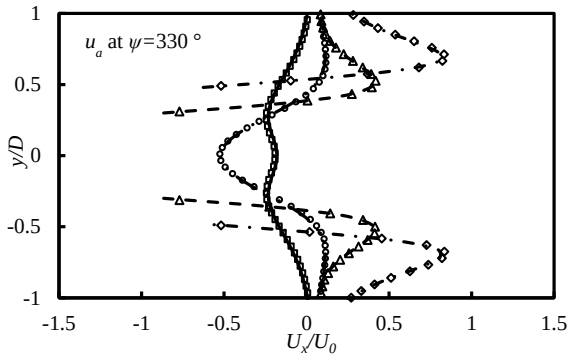

Figure 2. Comparison on velocity component between the present results (lines) and FEM numerical data (symbols) by Zhao and Cheng [6] for *KC* = 5, β = 20. □/—, ξ/D = -0.6; ◊/- -, ξ/D = 0.0; ○/-·-, ξ/D = 0.6; Δ/-···-··, ξ/D = 1.2. Coordinates transformed principles are list in Figure 4 from reference [6].

The numerical model was validated extensively against independent experimental and numerical results available in literature for oscillatory flow around a single cylinder [5], where good agreement with published force coefficients and flow regimes was reported. The validation checks will not be repeated here except that the velocity distributions of the present numerical results are compared with published data [6] in figure 2, where excellent agreement is achieved.

Flow Features

The flow features at Re = 150 are discussed here and are illustrated in figure 3 for different gap ratios and *KC*. The time history of the lift coefficients on cylinder 1 for selected *KC* and *G* are shown in figure 4, where $C_L = F_y / (\rho D U_m^2 / 2)$, with F_y being the force in the *y*-direction. At this Re, Tatsuno and Bearman [4] found regime A* and A for *KC* smaller than about 5.5, regime F for *KC* larger than approximately 7 (to beyond 12), and regime D between 5.5 and 7. In figure 3, the flow fields are visualized through streaklines in 10 oscillatory cycles, which are generated by releasing massless particles at 80 points around the cylinder surface with a frequency eight times of the flow oscillatory frequency.

For four staggered cylinders at $G = 1$, they behave similar to a single cylinder at most *KC* and the flow field at $KC \leq 5$ shows much similarity to regimes A* and A that were observed for a single cylinder [4]. The released particles are symmetrically distributed to the direction of motion when they are taken away by the oscillatory flow, even those released on the surfaces of two side cylinders 1 and 3 seem to be attracted to the centre line before being convected. However, the flow regime D, where the flow is obliquely convected to one side of the axis of oscillation by transverse vortex streets, is not present at $G = 1$, but rather the flow changes to regime F at $KC = 6$, where the flow is featured with two vortex streets aligned in a diagonal straight line at the two sides of the oscillatory axis, although the alignment angle is less than 5 °. A key observation at $KC = 7$ is that the streaklines bended in a way similar to regime C of a single cylinder, This observation is also evident in the time history of lift forces shown in figure 4(a), where a clear secondary period is found and it is about 7 times of the oscillatory periods. This rearrangement of vortices disappears at $KC = 8$, where the streaklines are distributed in a way of typical regime A. Beyond $KC \geq 9$ the flow fields tend to be chaotic and no regular features are readily identifiable.

For $G = 1$, it is observed from figure 4(a) that the force is very stable when $KC \leq 8$ while it is featured with random peaks at $KC = 9$ and 10. Very small lift coefficients are detected for $KC \leq 5$ because of the weakness of vortex shedding. The amplitude of lift coefficient is much larger at $KC = 5$, 6 and 7 than that at other *KC* because the vortex shedding from inner side of cylinder 1 and 3 is largely constrained at these cases, leading to much slimmer streaklines than, for instance, that at $KC = 8$ and 9. When *KC* exceeds 9, vortex shedding from each cylinder occurs and the interaction among these shed vortices also introduces turbulent features into the lift forces.

With increased gap distance at $G = 2$, the flow feature is very similar to $G = 1$ at the corresponding *KC*, but only the flow field turns to be turbulent at $KC \geq 8$. It should also be noted that at $KC = 6$, the fluid particles are convected in the same side to the oscillatory flow, similar to its counterpart in regime D for the single cylinder.

At larger gap distances, the flow usually quickly turns into turbulence with irregular flow fields, for instances, for $KC \geq 8$ at $G = 2$ and for $KC \geq 6$ at $G = 3$, and it is concluded from the three gap ratios that the flow fields are easier to be unstable at larger gap distances. The chaotic flow fields are due to the asymmetric state of vortex shedding from each cylinder, as it presents in regimes D, E and F for a single cylinder and also because of the interaction of the shed vortices in the confined space around the cylinders. The flow field is also increasingly unstable with the increase of Re. For instance, the flow field changes to be chaotic from $KC \geq 5$ at $G = 2$ and Re = 200. However, at low *KC* and/or Re, the four staggered cylinders present a symmetric flow flied. The released particles from two side cylinders (1&3) tend to be attracted by cylinders 2 and 4 and convected in the oscillatory direction. This flow feature is partially attributed to gap-vortex-shedding or gap flow between cylinder 2 and cylinder 1 or 3, which has been detailed in Zhao and Cheng [6] and Tong et al. [5]. It is seen from the present study that even in the staggered arrangements, the gap flow also plays a significant role in attracting fluids particles. As it is seen clearly from $KC = 5$ at $G = 3$, the attraction of gap flow between cylinders 1 and 2 induces bending streaklines to the two inline cylinders 2 and 4. As a result, the streaklines on the right hand of cylinder 1 create an inner-wards circulation zone, while the streaklines on the left hand of cylinder 1 also bend to the centre line when they are convected away.

Consistent with the observations on flow features at $G = 3$, the lift coefficients are featured with vagrant vibrations for $KC \geq 6$, embedded with randomly low and high vibrations. The relatively large amplitude of lift coefficient at $KC = 6$ and 7 and $G = 1$ disappears at $G = 3$ due to that the increased gap space releases the constrained vortex shedding from inner sides of cylinder 1. An interesting feature of unstable asymmetric vortex shedding is found at $KC = 7$. Between $50 < t/T < 75$, the mean lift is positive,

indicating the vortex shedding is only from the inner side of cylinder 1 and then are convected outwards, while from t/T = 75 onwards, the mean lift changes to be negative, suggesting a transition between the asymmetric direction in vortex shedding from the cylinder. This feature is similar to that observed in regime E around a single cylinder.

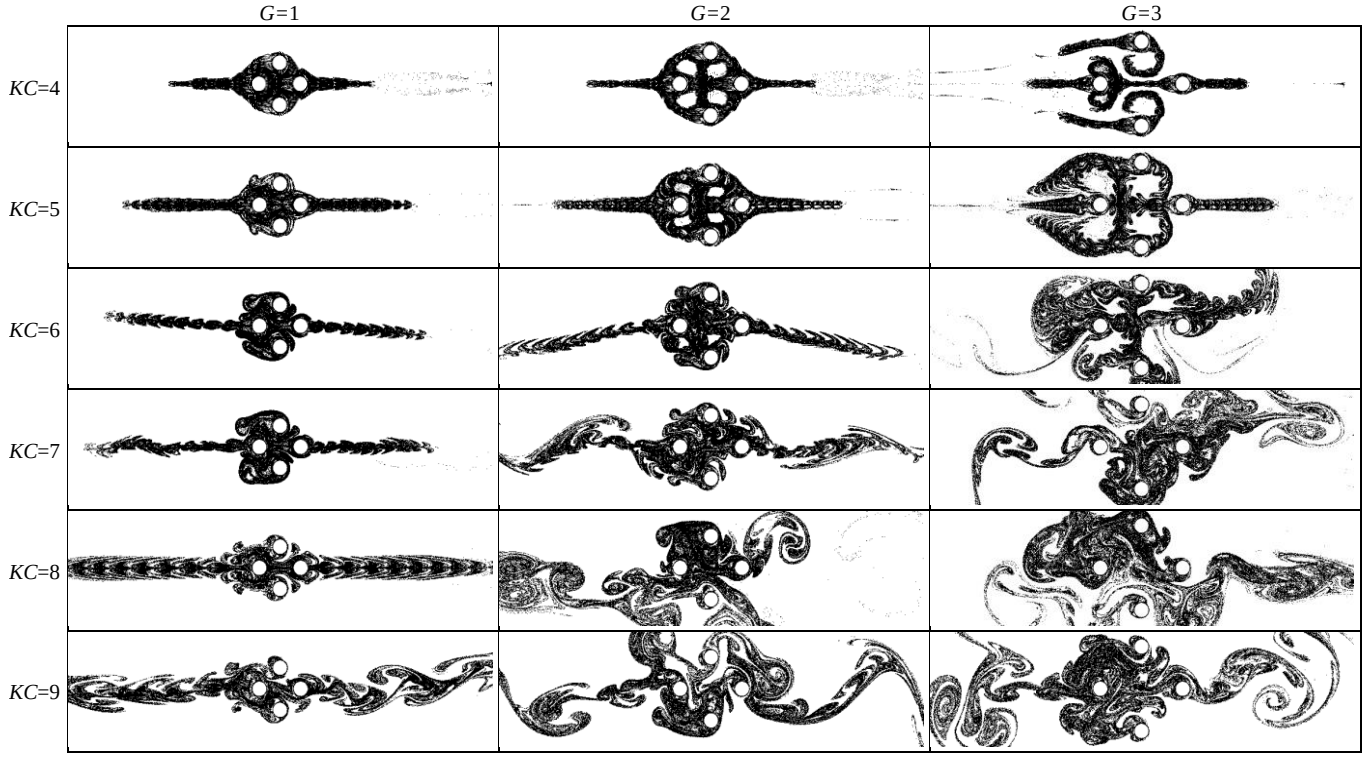

Figure 3. Simulated flow patterns represented by streaklines for oscillatory flow past four circular cylinders in diamond arrangemen at Re=150 and various *KC* and gap ratios.

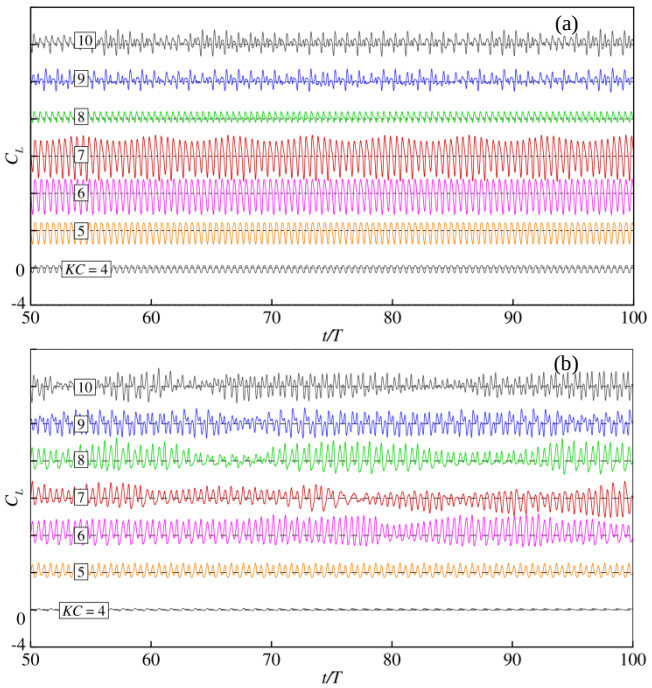

Figure 4. Time histories of the lift coefficient on cylinder 1 in the four staggered cylinders at various *KC* and Re = 150. (a) G = 1; (b), G = 3.

Force Coefficients

The calculated inertia and drag coefficients, C_M and C_D of cylinders 1 and 2 are compared with that of a single cylinder in the same flow condition in figure 5 (a&b), respectively. The drag and inertia coefficients are derived through the least square regression analysis of the inline force on the cylinder based on Morison equation,

$$F_x = \frac{1}{2}\rho D C_D |U_x(t)| U_x(t) + \rho \frac{\pi D^2}{4} C_M \frac{du(t)}{dt} \qquad (4)$$

where, F_x is the force on the cylindner in the inline direction and is obtained by integrating the pressure and shear stress along the cylinder surface.

One major observation is that the inertia and drag coefficients on cylinder 1 is larger than that on cylinder 2 at low *KC*, and from figure 5 it is observed that they are scattered on each side of the dashed lines, representing the force coefficients of a single cylinder. This is because of the wake sheilding effect, since cylinders 2 and 4 are in the wake of each other, resembling the drag reduction on the downstream cylinder of two tandem cylinders in steady flow. On the other hand, cylinders 1 and 3 not only directly face the incoming flow, but also are in the shear layers of cylinders 2 and 4, where significant high velocity is expected. However, this observation in the inline force coefficient experiences a dramatic change at *KC* larger than about 6, where the aymmetric vortex shedding make any regularity hard to be identified. But it is generally true that the drag coefficient on each cylinder in the staggered four is smaller than that of the single one at *KC* > 8, while the inertia coefficient is usually larger than that of the single cylinder.

The total root-mean-square (RMS) lift coefficient of the four cylinders and that on cylinder 1 are compared with those of a single cylinder in figure 6(a), where the total lift is divided by the number of the cylinders before the comparison. The magnitudes of the total lift force are significantly smaller than that of the single cylinder due to the fact that lift forces on cylinders 1 and 4 are usually in the opposite direction. The $C_{L\text{-}RMS}$ seems to rise with the enlarge of gap distances due to the increased vortex interactions. At *KC* = 8, where the vortex shedding from a single cylinder forms into regime F, the four staggered cylinders experience a drop in RMS lift coefficient as well, in agreement

with that of the single cylinder. This feature indicates that even the cylinders in close distance affect the flow field around each other and bring inidentifieable flow field at G = 2 and G = 3, they still behave independently to a certain extent. In contrast, any member cylinders in the diamond arranged four cylinders experiences quite large magnitude of lift forces, which is evident from the time history of lift forces as shown in figure 4(a).

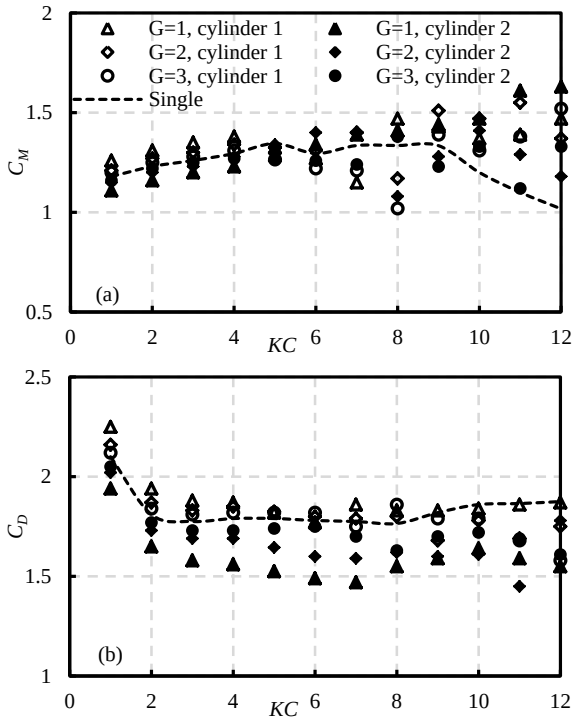

Figure 5. Inertial and Drag coefficients on two selected members in the array of four staggered cylinders compared to those of a single one under the same flow condition.

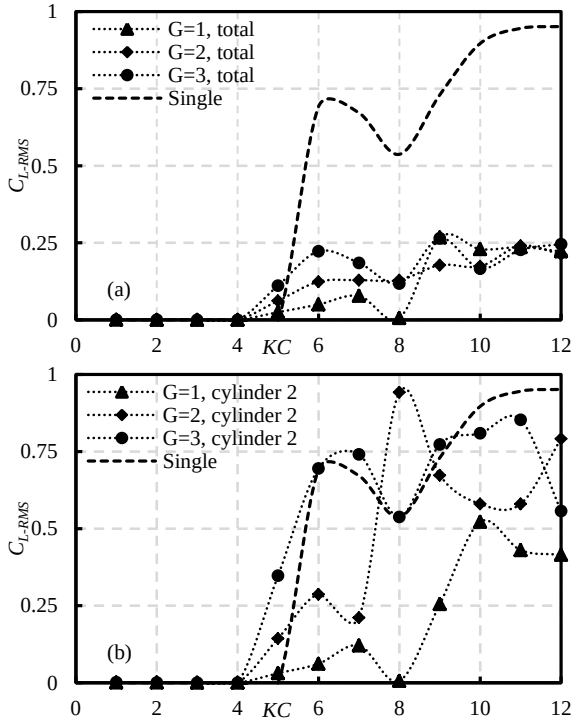

Figure 6. Comparison of the RMS lift forces on cylinder 1 (a) and on the array as a whole (b) with those of a single cylinder at Re=150.

Figure 6 (b) illustrate the RMS lift coefficient on cylinder 2. It is observed that the trend of variations of lift on cylinder 2 generally agree with that of the total forces as shown in figure 6(a). Although the lift on cylinder 2 is still small at most *KC*, the magnitude is much more comparable to that of the single cylinder.

Conclusions

This study investigates the features of oscillatory flow around four circular cylinders in a diamond arrangement and their impact on forces on these structures. At close distances and low frequencies of oscillation, the flow field around four staggered cylinders resemble that around a single cylinder, and regimes A, A*, D and regime F are detected, however, usually at a *KC* number different from that of a single cylinder.

The interferences of the four cylinders also present symmetric flow fields to the direction of inlet flow, which are mainly found at *KC* numbers in regime A for a single cylinder. The massless particles released from the two sides of the cylinders usually attracted by the gap flow to the centred two cylinders before being convected away.

It is found that when cylinders are placed in staggered arrangements, the flow field is prone to be chaotic due to the influences of asymmetric vortex shedding from each member and the interactions of the shed vortices. The flow field becomes increasedly unstable with the increased gap distances as well as increased Re.

The two inline cylinders generally experience low drag and inertial force coefficients compared to that of two side-by-side cylinders, partially due to the wake shielding effect and to the fact that the side cylinders are in the shear layer of the two centred ones.

Acknowledgments

This work was supported by Australian Research Council Discovery Grant (Project ID: DP110105171) and by iVEC through the use of advanced computing resources (Epic and Magnus supercomputers).

References

[1] An, H., Cheng, L. & Zhao, M., Direct numerical simulation of oscillatory flow around a circular cylinder at low Keulegan–Carpenter number. *J. Fluid Mech.*, **666**, 2011, 77-103.

[2] Chern, M. J., Shiu, W. C. & Horng, T. L., Immersed boundary modeling for interaction of oscillatory flow with cylinder array under effects of flow direction and cylinder arrangement. *J. Fluids Struct.*, **43,** 2013, 325-346.

[3] Sarpkaya, T., Experiments on the stability of sinusoidal flow over a circular cylinder. *J. Fluid Mech.*, **457,** 2002, 157-180.

[4] Tatsuno, M. & Bearman, P., A visual study of the flow around an oscillating circular cylinder at low Keulegan–Carpenter numbers and low Stokes numbers. *J. Fluid Mech.*, **211,** 1990, 157-182.

[5] Tong, F., Cheng, L., Zhao, M. & An H., Oscillatory flow regimes around four cylinders in a square arrangement under small *KC* and Re conditions, *J. Fluid Mech.*, under revision.

[6] Zhao, M. & Cheng, L., Vortex shedding regimes of oscillatory flow past two circular cylinders in side-by-side and tandem arrangements at low Reynolds number, *J. Fluid Mech.*,**751**, 2014, 1-37.